are minimized, in agreement with the theoretical calculations and the photoelectron measurements.

The observation that the first oxidation potential changes more with changing solvent than the second oxidation potential also explains the reduction of ΔE with increasing solvating power of solvent. The linear relationship observed for the ΔE values for the three compounds shows that differences between $E2$ and $E1$ have the same solvent dependence and are therefore likely to be mostly charge dependent. As mentioned above, the ΔE values for BEDO and BEDT are virtually identical for any given solvent.[24] By contrast, the values of ΔE(TTF) are consistently around 0.1 V higher than the corresponding BEDO and BEDT values. It follows that TTF^+ is stabilized to a greater extent by the solvent–electrolyte combination than are $BEDO^+$ or $BEDT^+$.

Conclusions

The PES results indicate that, in agreement with theoretical models, substituting the terminal hydrogen atoms of TTF by electron- (π-) donating oxygen atoms does lead to a reduction of the first IP, while substitution by sulfur makes almost no difference. The electrochemical studies, however, have revealed that solvent effects play a large part in determining the relative ease of oxidizing TTF and its derivatives in solution. It is likely that the ability of TTF derivatives to function as electron donors in the solid state will also depend critically on their environment in the solid and the extent to which they are "solvated" by themselves and by the acceptor molecules. Interestingly, as this work was being submitted, such factors were identified in a comprehensive study of a pthalocyanine molecular metal reported in this journal by Marks and co-workers.[25]

Acknowledgment. D.L.L. acknowledges support by the U.S. Department of Energy (Division of Chemical Sciences, Office of Basic Energy Sciences, Office of Energy Research, DE-FG02-86ER13501), the National Science Foundation (CHE85-19560), and the Materials Characterization Program, Department of Chemistry, University of Arizona. R.L.J. thanks the Science and Engineering Research Council (U.K.) for the award of a NATO postdoctoral fellowship. He also thanks Dr. Anjana Rai-Chaudhuri for helpful discussions and Swati Chattopadhyay for help in assembling some of the figures. F.W. acknowledges support by the National Science Foundation (DMR88-20933).

Registry No. 1a, 31366-25-3; **1b**, 120120-58-3; **1c**, 66946-48-3; **2**, 125996-97-6.

(24) A reviewer suggested that in the dications "the two five-membered rings twist [by] ca. 90° [relative] to one another. This would have the effect of increasing the coefficients on the "outer" carbons in the HOMO, thereby allowing more resonance stabilization by the oxygens in BEDO".

(25) (a) Gaudiello, J. G.; Kellogg, G. E.; Tetrick, S. M.; Marks, T. J. *J. Am. Chem. Soc.* **1989**, *111*, 5259. (b) Almeida, M.; Gaudiello, J. G.; Kellogg, G. E.; Tetrick, S. M.; Marty, H. O.; McCarthy, W. J.; Butler, J. C.; Kannewurf, C. R.; Marks, T. J. *J. Am. Chem. Soc.* **1989**, *111*, 5271.

A Theoretical Approach to Drug Design. 1. Relative Solvation Thermodynamics for the Antibacterial Compound Trimethoprim and Ethyl Derivatives Substituted at the 3′, 4′, and 5′ Positions

Charles L. Brooks III*,† and Stephen H. Fleischman‡

Contribution from the Department of Chemistry, Carnegie Mellon University, Pittsburgh, Pennsylvania 15213, and Convex Computer Corporation, Richardson, Texas 75080.
Received September 18, 1989

Abstract: Free energy simulation methods are used to compute the relative solvation thermodynamics of the antibacterial drug trimethoprim [2,4-diamino-5-(3′,4′,5′-trimethoxybenzyl)pyrimidine] and a family of congeners derived from methoxy → ethyl substitution on the benzyl ring. The aqueous solubility is found to decrease as more hydrophobic character is introduced into the parent molecule. Nearly additive effects on the solvation free energy are observed for the mono- and disubstituted derivatives, with exception of the 3′,5′-diethyl derivative. This compound shows an increased aqueous solubility (over that of the other diethyl compound), which is linked to anomalous entropic effects of the *p*-methoxy group. The triethyl-substituted molecule exhibits a similar solvation free energy to that of the 3′,4′-diethyl compound, which appears as additive contributions from the 3′,5′-diethyl and 4′-monoethyl derivatives.

I. Introduction

The thermodynamics of solvation play a critical role in understanding molecular association. For example, consider the "drug design" paradigm, which involves the *relative* thermodynamics for the inhibitor displacement reaction

$$I_b(aq) + E{:}I_a \rightleftharpoons I_a(aq) + E{:}I_b \qquad (1)$$

In this reaction, inhibitor a (I_a) is initially bound to the receptor (enzyme, E), and inhibitor b (I_b) is present in aqueous solution. Inhibitor b is then *desolvated* and a is *solvated*, with the overall change in binding affinity being attributed to the *relative solvation* thermodynamics of a versus b, as well as the *relative interaction* thermodynamics with the receptor E. The objective in studying this process, as viewed from the drug design paradigm, is to optimize (or to find some strategy to optimize) certain characteristics of the interaction of I_b with E compared to I_a with E. The overall success of this procedure requires knowledge of inhibitor–enzyme interactions and aqueous solubilities. Thus, understanding solvation thermodynamics is crucial to the development of detailed models for the rationalization and prediction of inhibitor binding.

Computer simulation methodologies developed over the past several years[1,2] now serve as an aid in the molecular interpretation

† Carnegie Mellon University.
‡ Convex Computer Corp.

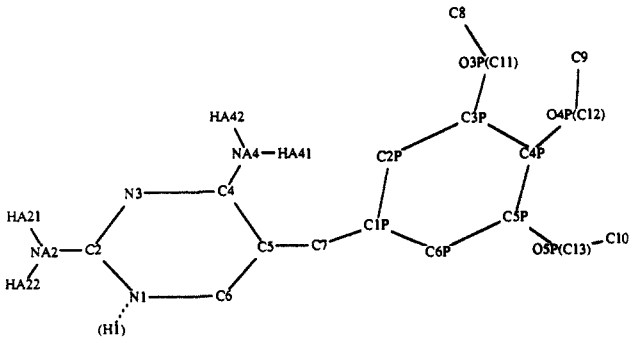

Figure 1. Molecular topology and atom names for trimethoprim and its ethyl-substituted congeners.

of solvation and interaction thermodynamics involved in inhibitor displacement reactions such as those given in eq 1. These techniques provide an exciting new approach for the development and exploration of drug design strategies. Key to the application of computational methods to this problem has been the implementation of thermodynamic simulation techniques,[3] particularly thermodynamic cycle perturbation theory.[4] This approach may be applied to compute thermodynamics for the individual processes

$$I_b(aq) \rightleftharpoons I_a(aq) \tag{2}$$

and

$$E{:}I_a \rightleftharpoons E{:}I_b, \tag{3}$$

which, when combined in a closed thermodynamic cycle, yield the thermodynamic state functions associated with the reaction of eq 1.[5] The first of the above two processes is related to the aqueous solvation thermodynamics. When the additional gas-phase process is considered

$$I_a(vac) \rightleftharpoons I_b(vac) \tag{4}$$

the relative solubility of I_a compared to I_b may be obtained.

In this paper we will focus on the solvation thermodynamics for a specific system, trimethoprim [2,4-diamino-5-(3′,4′,5′-trimethoxybenzyl)pyrimidine] and the five unique congeners that arise from combinations and permutations of the methoxy → ethyl substitutions at the meta and para positions of trimethoprim's benzyl ring (see Figure 1). (Note that symmetry due to rotations around the C7–C1′ bond in this drug make the 3′ and 5′, and the 3′,4′ and 4′,5′ substitutions identical in solution.) In a companion paper to be published shortly, the interaction thermodynamics between these compounds and the enzyme dihydrofolate reductase (from chicken) will be considered.[6,7] This combined work will illustrate the systematic application of thermodynamic simulation methods to drug design problems, that is, rationalization/optimization of guest–host interaction thermodynamics.

Trimethoprim (TMP) and the dihydrofolate reductase (DHFR) system are of pharmacological and medical importance. The binding of small drugs, like trimethoprim, to the enzyme dihydrofolate reductase is an important means of combating bacterial infections in humans. This is due to the 600–1000-fold greater affinity of TMP for the bacterial versus the mammalian enzyme[6] that preferentially reduces cellular proliferation of guest bacteria. In addition, the inhibition of DHFR by methotrexate (a related nitrogen heterocycle) is an important chemical means of controlling some cancerous cell growth. Both of these compounds are effective in their action because they inhibit (sometimes preferentially) the central activity of DHFR, which is the synthesis of peptide and nucleotide precursors.[8] It is for this reason that many previous experimental and theoretical studies have focused on DHFR and compounds effective in its inhibition.[6-10] This wealth of background information and the practical importance of DHFR inhibitory drugs provide key motivations for our work.

In the remainder of this paper we will present and discuss the results of our calculations of the relative solvation thermodynamics for trimethoprim and its congeners. In the next section we will outline the methods and models we have employed. Following this we will present results for the relative hydration free energies, entropies, and energies of these five trimethoprim-related compounds, with a discussion of the observed behavior and a comparison of solvation thermodynamics for methoxy-substituted benzenes,[11] which can be viewed as a model for TMP congeners. We conclude with an overview of our findings.

II. Methods and Models

Thermodynamic simulation methods have been employed in a number of previous studies and the details are already present in the literature.[3,5] For this reason we provide only a listing of the connection formula that we used to compute free energies, energies, and entropies.

In order to transform one molecule into another we use the thermodynamic mapping Hamiltonian given by

$$H(\lambda) = (1 - \lambda)H_R + \lambda H_P + H_{env} \tag{5}$$

where H_R is the Hamiltonian for the "reactant", e.g., those portions of the molecule I_b given in eq 2 that change their chemical identity; H_p is the "product" Hamiltonian; H_{env} is the environment Hamiltonian, which represents the aqueous solvent and/or those portions of molecules I_b and I_a that are chemically identical; and λ is an advancement coordinate that carries the reaction between the reactant and product states. Using this Hamiltonian, we can define equations of motion for the hybrid system at any value of λ and use molecular dynamics to generate an ensemble of configurations for the system. We note that our implementation of these equations of motion strictly uses the Hamiltonian as given in eq 5; i.e., we directly scale overall energy terms and do not scale individual parameters.[5,12]

From this ensemble of configurations we compute the statistical mechanical connection formula

$$\Delta A(\lambda,\lambda') = -\beta^{-1} \ln \langle \exp[-\beta\{H(\lambda') - H(\lambda)\}] \rangle_\lambda \tag{6}$$

to yield the free energy difference between states defined by $H(\lambda)$ and $H(\lambda')$; here β is $1/k_BT$, k_B is Boltzmann's constant, and T is the absolute temperature. Individual simulations are carried out for several values of λ (3–4 "windows" in all cases considered here), covering the range (0,1), and the overall free energy change is constructed as the sum of these values. Identical calculations are performed for the molecules in aqueous solution and in a vacuum, and the difference yields the relative solvation free energy.[5]

Entropy and energy changes are computed by directly utilizing the precision available in eq 6 to construct finite-difference temperature derivatives.[5] The relevant equation for the entropy is

$$\Delta S(\lambda,\lambda') = -\frac{\Delta A(\lambda,\lambda')}{T} + \frac{1}{2\beta\delta T} \ln \left\{ \frac{\langle \exp[-\beta_+ H(\lambda') + \beta H(\lambda)] \rangle_{\lambda,T} \langle \exp[-\gamma_- H(\lambda)] \rangle_{\lambda,T}}{\langle \exp[-\beta_- H(\lambda') + \beta H(\lambda)] \rangle_{\lambda,T} \langle \exp[-\gamma_+ H(\lambda)] \rangle_{\lambda,T}} \right\} \tag{7}$$

(1) References 1 and 2 provide a general review of simulation methods applied to biological molecules. Brooks, C. L., III; Karplus, M.; Pettitt, M. B. In *Proteins: A Theoretical Perspective on Structure Dynamics and Thermodynamics. Adv. Chem. Phys.* **1988**, *79*.

(2) McCammon, J. A.; Harvey, S. *Dynamics of Proteins and Nucleic Acids*; Cambridge, University Press: Cambridge, 1987.

(3) See Beveridge, D. L.; DiCapua, F. M. *Annu. Rev. Biophys. Chem.* **1989**, *18*, 431 and references therein for a review of free energy simulation methods and applications.

(4) Tembe, B. L.; McCammon, J. A. *Comput. Chem.* **1984**, *8*, 281.

(5) For a recent review of our methods, see: Brooks, C. L., III. *Int. J. Quant. Chem.: Quant. Biol. Symp.* **1988**, *15*, 221.

(6) Matthews, D. A.; Bolin, J. T.; Burridge, J. M.; Filman, D. J.; Volz, K. W.; Kaufman, B. T.; Beddell, C. R.; Champness, J. M.; Stammers, D. K.; Kraut, J. *J. Biol. Chem.* **1985**, *260*, 381. Matthews, D. A.; Bolin, J. T.; Burridge, J. M.; Filman, D. J.; Volz, K. W.; Kraut, J. *J. Biol. Chem.* **1985**, *260*, 392.

(7) Li, R.; Hansch, C.; Matthews, D.; Blaney, J. M.; Langridge, R.; Delcamp, T. J.; Susten, S. S.; Freisheim, J. H. *Quant. Struct.-Act. Relat. Pharmacol. Chem. Biol.* **1982**, *1*, 1.

(8) Cody, V.; Sutton, P. A. *J. Am. Chem. Soc.* **1988**, *110*, 6219.

(9) Kuyper, L.; Roth, B.; Baccanari, D. P.; Ferone, R.; Beddell, C. R.; Champness, J. N.; Stammers, D. K.; Dann, J. G.; Norrington, F. E.; Haker, D. J.; Goodford, P. J. *J. Med. Chem.* **1985**, *28*, 303.

(10) (a) Singh, U. C. *Proc. Natl. Acad. Sci. U.S.A.* **1988**, *85*, 4280. (b) Singh, U. C.; Benkovic, S. J. *Proc. Natl. Acad. Sci. U.S.A.* **1988**, *85*, 9519.

(11) Kuyper, L.; Ashton, D.; Merz, K. M.; Kollman, P. *J. Phys. Chem.*, in press.

(12) Bash, P. A.; Singh, U. C.; Brown, F. K.; Langridge, R.; Kollman, P. A. *Science* **1987**, *235*, 574.

where $\beta_{\pm} = [k_B(T \pm \delta T)]^{-1}$, $\gamma_{\pm} = \beta_{\pm} - \beta$, and δT is the temperature increment used to compute the finite-difference derivative (10 °C in the present cases). The energy is computed from the thermodynamic relationship

$$\Delta E(\lambda,\lambda') = \Delta A(\lambda,\lambda') + T\Delta S(\lambda,\lambda') \quad (8)$$

With these expressions $\Delta\Delta S$ and $\Delta\Delta E$ are constructed in a fashion analogous to $\Delta\Delta A$.

In all of the results from eq 6–8 estimates of statistical error (precision) are made by using the method of batch means.[13] A uniform bin size of 1000 steps was used throughout the calculations. This represents a compromise between the much larger bin sizes necessary to estimate the statistical precision of $\Delta\Delta S$ and $\Delta\Delta E$ and the smaller bin sizes adequate for $\Delta\Delta A$. Our focus is on free energy changes; therefore, this protocol is optimized for those calculations.

The molecular simulations of trimethoprim and its ethyl-substituted congeners in aqueous solution and vacuum were carried out with our highly modified and optimized version of the macromolecule simulation package CHARMM.[14] All simulations used a time step of 1.5 fs and employed the SHAKE algorithm[15] to constrain heavy atom–hydrogen bonds. The aqueous systems representing drug plus water consisted of 196 three-site water molecules and the hybrid drug. The parameters and geometry describing the drug molecules are given in Table I and Figure 1. The solvent was represented by the three-site TIP3P water model fo Jorgensen,[14] and the solute–solvent van der Waals interactions were constructed by using a geometric mean combination rule for ϵ_{min} and an arithmetic mean for R_{min}. The bonded and nonbonded parameters were constructed to be consistent with the CHARMM (PARAM19) parameter set[15] by direct comparison with analogous fragments in the CHARMM parameter library. Minimum image periodic boundary conditions with an atom-based spherical cutoff to 8.5 Å for van der Waals and electrostatic interactions were employed. The size of the cubic box was adjusted to give a solvent density near 1 g/cm^3, and the temperature was maintained near 298 K by coupling all non-hydrogen atoms to a Langevin heat bath.[16]

In the calculation of relative solvation thermodynamics for the *p*-ethyl and the triethyl substitution, simulations were performed at each value of λ for 20 ps of equilibration and 30 ps of production, during which time the energies necessary for calculation of the various thermodynamic quantities were saved and subsequently processed. These simulations were run with λ = (0.125, 0.5, and 0.875) using double-wide sampling (two values of λ' per simulation) to span the entire λ space. An additional λ window at λ = 0.969 was added for the 4′-ethyl substitution, the 3′,4′-diethyl substitution, and the 3′,5′-diethyl substitution; otherwise the simulations were analogous to those just described. The additional window was added in anticipation that more sampling was necessary for the aqueous-phase calculations near λ = 1. However, this proved not to be the case since free energies computed with only three double-wide windows gave very similar results. Finally, we note that all perturbation calculations used trimethoprim as the reference structure.

III. Results and Discussion

The replacement of relatively hydrophilic (methoxy) groups by more hydrophobic (ethyl) ones on the benzyl ring of trimethoprim should decrease its aqueous solubility as measured by the transfer free energy from the ideal gas phase to an aqueous environment. We are interested in examining whether or not this increasing solvation free energy is additive for the replacement of one, two, or three methoxy moieties on TMP. Previous measurements of the influence of *adding* methoxy groups to benzene show that the incremental decrease in free energy is nearly additive.[11] It will be interesting to compare this finding, which conversely suggests that removal of methoxy groups from trimethoprim should yield additive *increments* in solvation free energy, with ours for the replacement of methoxy by ethyl. Our results are summarized in Table II and in Figure 2.

In Table II we give the component aqueous and vacuum free energies, energies, and entropies necessary to construct the solvation thermodynamics (aqueous property minus vacuum) along with our estimates of their statistical precision. As is obvious from these results, the free energies are quite precise, whereas the component energies and entropies are not. This results primarily because energy and entropy are derivatives of the free energy and converge more slowly than the free energy itself.

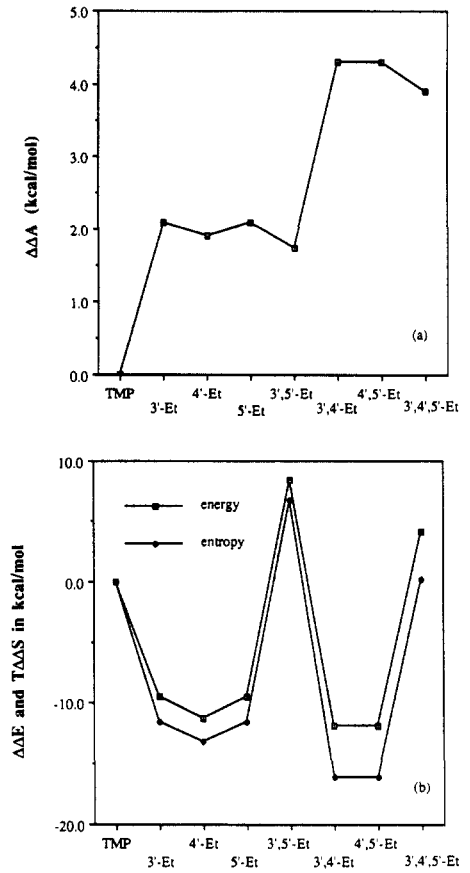

Figure 2. Solvation thermodynamics for trimethoprim congeners: (a) free energy of solvation ($\Delta\Delta A_{solv}$) in aqueous solution relative to trimethoprim; (b) energy ($\Delta\Delta E_{solv}$) and entropy ($\Delta\Delta S_{solv}$) of solvation in aqueous solution relative to trimethoprim.

In addition to estimating the statistical precision by calculation of the standard deviation of bin averages, we have repeated various simulations at specific values of λ for a few of the aqueous legs of the calculation using identical control parameters but generating independent initial velocities and starting configurations. This is probably a better estimate of the "repeatability" of the calculation (measurement), but is not always feasible to carry out because of the computational expense. Our finding from these calculations indicates that the overall free energy determinations are repeatable to within a few tenths of a kcal/mol and the overall energy determinations are precise to 3–5 kcal/mol. These determinations are consistent with our calculated estimates of precision based on bin averages. Therefore, we conclude that the use of bin averages and their standard deviations are sufficient reflections of the repeatability of our calculations. We also note that because the energy and entropy are much less precise than the free energy, we will use these properties only in a qualitative way to reinforce our interpretations of the free energy results.

Another interesting test is to determine to what extent a closed thermodynamic cycle is achieved in a series of mutation calculations. To examine this question we have carried out a calculation of the relative solvation free energy of the diethyl derivative (3′,5′) compared to the triethyl compound directly, i.e., without referencing both to trimethoprim. From this set of calculations, aqueous and vacuum legs of the thermodynamic cycle, we find the triethyl derivative to have a solvation free energy 1.5 kcal/mol more positive than that of the 3′,5′ species. This is to be compared with the 2.1 kcal/mol obtained from the results presented in Table II. A significant disparity between these two numbers would be

(13) Schiferel, S. K.; Wallace, D. C. *J. Chem. Phys.* **1985**, *83*, 5203.
(14) Jorgensen, W. L.; Chandrasekhar, J.; Madura, J. D.; Impey, R. W.; Klein, M. L. *J. Chem. Phys.* **1983**, *79*, 926.
(15) Brooks, B. R.; Bruccoleri, R. E.; Olafson, B. D.; States, D. J.; Swaminathan, S.; Karplus, M. *J. Comput. Chem.* **1983**, *4*, 187.
(16) Rychaert, J. P.; Ciccotti, G.; Berendsen, H. J. C. *J. Comput. Phys.* **1977**, *23*, 327.
(17) Brunger, A.; Brooks, C. L., III; Karplus, M. *Chem. Phys. Lett.* **1984**, *105*, 495.

Table I. Molecular Mechanics Parameters for Trimethoprim and Its Congeners[a]

Bond Parameters

		k_c, kcal/(mol·Å^2)	r_{eq}, Å			k_c, kcal/(mol·Å^2)	r_{eq}, Å
CA	CA	450.0	1.380	N2	CA	400.0	1.333
CA	CR1E	450.0	1.380	NC	CA	400.0	1.339
CA	CH2E	405.0	1.520	CA	OS	450.0	1.380
H2	N2	472.0	1.010	HC	NC	405.0	1.000

Angle Parameters

			k_c, kcal/(mol·rad^2)	θ_0, deg				k_c, kcal/(mol·rad^2)	θ_0, deg
CA	CA	CA	70.0	120.0	CA	CH2E	CA	70.0	109.5
CA	CA	CH2E	65.0	126.5	CA	CH2E	CH3E	70.0	113.0
CA	CA	CR1E	70.0	120.0	CA	CR1E	CA	70.0	120.0
CA	CA	N2	70.0	123.5	CA	CR1E	CR1E	70.0	120.0
CA	CA	NC	70.0	117.3	CA	NC	CR1E	70.0	118.6
CA	CA	OS	70.0	119.0	CA	NC	CA	70.0	118.6
CH2E	CA	CR1E	70.0	121.0	CA	OS	CH3E	46.5	120.5
CR1E	CA	CR1E	70.0	120.0	CA	NC	HC	35.0	120.0
CR1E	CA	OS	70.0	119.0	CR1E	NC	HC	35.0	120.0
NC	CA	NC	70.0	129.1					

Dihedral Angle Parameters

				k_c, kcal/mol	p^b (periodicity)	ϕ_0, deg					k_c, kcal/mol	p^b (periodicity)	ϕ_0, deg
X	CA	CH2E	X[c]	0.0	3	0.0	CA	CA	OS	CH3E	1.732	2	180.0
CR1E	CA	OS	CH3E	1.732	2	180.0							

Improper Dihedral Angle Parameters

				k_c, kcal/mol	ϕ_0, deg					k_c, kcal/mol	ϕ_0, deg
CR1E	X	X	NC	25.0	0.0	CR1E	X	X	OS	150.0	0.0
CR1E	X	X	N2	43.0	0.0	CA	X	X	OS	150.0	0.0
CA	X	X	CA	25.0	0.0	CA	X	X	CH2E	90.0	0.0
CA	X	X	CR1E	25.0	0.0	NC	X	X	HC	45.0	0.0

Nonbonded Parameters

	ϵ_{min}, kcal/mol	$R_{min}/2$, Å		ϵ_{min}, kcal/mol	$R_{min}/2$, Å
H2	−0.0498	0.800	CH2E[d]	−0.1142	2.235
HC	−0.0498	0.600	CH3E	−0.1811	2.165
N2	−0.2384	1.600	CR1E	−0.1200	2.100
NC	−0.2384	1.600	CA	−0.1200	2.100
OS	−0.1591	1.600			

TIP3P Water Nonbonded Parameters[14]

		ϵ_{min}, kcal/mol	R_{min}, Å			ϵ_{min}, kcal/mol	R_{min}, Å
OT	OT	−0.152073	3.5365	HT	OT	−0.08363	1.9927
HT	HT	−0.04598	0.4490				

Atomic Charges for Trimethoprim and Congeners

atoms[e]	unprotonated	protonated	atoms[e]	unprotonated	protonated
H1		0.3	NA4	−0.42	−0.42
N1	−0.3	0.0	HA41, HA42	0.21	0.21
C2	0.4	0.5	C7	0.0	0.0
N3	−0.3	−0.3	C1P, C2P, C6P	0.0	0.0
C4	0.2	0.25	O3P, O4P, O5P	−0.3	−0.3
C5	0.0	0.05	C3P, C4P, C5P	0.15 (0.0)[f]	0.15 (0.0)
C6	0.0	0.1	C8, C9, C10	0.15 (0.0)	0.15 (0.0)
NA2	−0.42	−0.37	C11, C12, C13	—, (0.0)	—, (0.0)
HA21, HA22	0.21	0.21			

[a] Parameters are in the standard CHARMM format.[15] [b] p is the periodicity of the cosine series for the dihedral angle potential. [c] X denotes a wildcard specifier for dihedral angle parameters. [d] All carbons interacting through 1–4 nonbonded interactions use the parameters ϵ_{min} = 0.1 kcal/mol and $R_{min}/2$ = 1.9 Å. [e] Atomic charges for atoms as indicated in Figure 1. Atom types corresponding to names are as follows: C2, C4, C5, C1P, C3P, C4P, and C5P are of type CA; NA2 and NA4 are of type N2; HA21, HA22, HA41, and HA42 are of type H2; N1 is of type NC; C6, C2P, and C6P are of type CR1E; O3P, O4P, and O5P are of type OS; C7, C11, C12, and C13 are of type CH2E; C8, C9, and C10 are of type CH3E. Atom H1 is of type HC but is not used in simulations of TMP (or congeners) in aqueous solution where the molecule is unprotonated at normal pH. [f] Numbers in parentheses represent charges on ethyl derivative atoms.

indicative of incomplete thermodynamic sampling; the observed agreement is well within the range of expected differences between separate free energy determinations, and therefore we again reach the conclusion that we have carried out sufficient sampling.

We now turn to the relative solvation free energy for TMP's congeners. These are displayed in Figure 2a and Table III. A clear trend is evident from the figure and may be summarized as follows: the monoethyl substitutions all decrease the solubility

Table II. Component Thermodynamics for Trimethoprim Congeners[a]

system		ΔA	ΔE	$T\Delta S$[b]
3′- or 5′-monoethyl	(a)[c]	−1.5 ± 0.1	−12.4 ± 5	−10.9 ± 5
derivative	(v)[d]	−3.5 ± 0.2	−2.9 ± 4	0.6 ± 4
4′-monoethyl	(a)	−1.5 ± 0.2	−16.5 ± 5	−15.0 ± 5
derivative	(v)	−3.4 ± 0.1	−5.2 ± 2	−1.8 ± 2
3′,4′- or 4′,5′-diethyl	(a)	−2.4 ± 0.3	−18.6 ± 7	−16.2 ± 7
derivative	(v)	−6.7 ± 0.4	−6.8 ± 9	−0.1 ± 9
3′,5′-diethyl	(a)	−2.1 ± 0.2	4.1 ± 6	6.2 ± 6
derivative	(v)	−3.9 ± 0.2	−4.3 ± 4	−0.5 ± 4
3′,4′,5′-triethyl	(a)	−4.9 ± 0.3	−2.7 ± 6	2.2 ± 6
derivative	(v)	−8.8 ± 0.4	−6.8 ± 9	2.0 ± 9

[a] All thermodynamic properties are reported in kcal/mol; error estimates represent standard deviations of mean by method of batch means. [b] Temperature used was 298 K. [c] Calculations for aqueous-phase leg of thermodynamic cycle (eq 3). [d] Calculation for gas-phase leg of thermodynamic cycle (eq 4).

Table III. Comparison of Relative Solvation Free Energy for Trimethoprim and Methoxybenzene Derivatives[a]

no. of methoxy groups	rel free energy, kcal/mol	
	trimethorpim derivs $\Delta\Delta A_{solv}$	1,2,3-trimethoxybenzene derivs $\Delta\Delta G_{solv}$
2	2.0 ± 0.2 (1.9 ± 0.2)[b]	1.68[c]
1	4.3 ± 0.3 (1.8 ± 0.3)[d]	3.03
0	3.9 ± 0.5	4.54

[a] Data constructed from solubility measurements of ref 11. [b] Value in parentheses is for 4′-monoethyl derivative. [c] Value is for 1,2-dimethoxybenzene compared to 1,2,3-trimethoxybenzene. [d] Value in parentheses is for 3′,5′-diethyl derivative.

with attendant free energy increases of about 2 kcal/mol; the diethyl derivatives fall into two groups, one at 4.3 kcal/mol and one at 1.8 kcal/mol; and the triethyl derivative is at 3.9 kcal/mol relative to trimethoprim. The position of the ethyl derivativization has only a small influence on the change in solvation free energy for the single ethyl derivatives as can be seen in Table III. However, when two of the methoxy groups are changed to ethyl groups, there is a positional effect, with the 3′,4′ derivative yielding a more positive solvation free energy than the 3′,5′ derivative. This difference is linked to large energy and entropy components for the aqueous solution portion of the overall solvation cycle (see eq 3 and Table II) which occurs when the methoxy group remains in the para position while two ethyl groups flank it. (Differences are also evident in the gas-phase (or vacuum) portion of the calculations. These differences are largely due to the bonded (bonds, angles, and dihedral) free energy contributions and for the most part cancel when the complete solvation cycle is constructed.) Our observation, that the 3′,5′-diethyl derivative is about as soluble as single ethyl derivatives of TMP, may be a reflection of the increased hydrophilicity of the *p*-methoxy group observed in water–octanol partition coefficient measurements.[18] If this is so, our results suggest that entropy is at the origin of this influence and that it yields a qualitatively different contribution to the solvation free energy, which is consistent with the greater hydrophilicity of the *p*-methoxy. This is evident in the results displayed in Figure 2b, which shows a favorable entropic contribution to the solvation free energy for this compound. The triethyl derivative of trimethoprim also shows greater hydrophilic character in the entropic term. This is indicated by the small entropic contribution, compared with the other congeners exclusive of the 3′,5′-diethyl derivative. This trend is also evident in Figure 2.

Next we discuss the incremental additivity of the solvation free energy for the ethyl derivatives. The 3′,4′-diethyl derivative of trimethoprim has slightly more than twice the solvation free energy of the monoethyl compounds. This can be considered to be, essentially, additive increments from the 3′ and 4′ derivatives. The 3′,5′-diethyl derivative, on the other hand, has a solvation free energy similar to that of the monoethyl derivatives and is clearly not additive. This is due to the increased hydrophilicity of the *p*-methoxy group as noted above. The solvation free energy for the triethyl derivative appears to be composed of additive increments of the 3′,5′-diethyl compound and the 4′-monoethyl compound. It is interesting to note that simple additivity does not hold for the calculations presented here. However, when the diethyl congeners are broken into the two groups, it appears that the 3′,4′ (4′,5′) derivative is related to the monoethyl derivative in an additive fashion and the triethyl congener is related to the 3′,5′ and 4′ derivatives.

One may also ask how these findings compare with results of solubility measurements on methoxybenzenes and other related compounds. A recent set of experiments have provided new data on the solubilities of 1,2,3-trimethoxybenzene, 1,2-dimethoxybenzene, anisole, and benzene.[11] The results from these measurements are reproduced in Table II. In this series of compounds one, two, or three methoxy groups are replaced by hydrogen, similar to the replacements of methoxy by ethyl groups in trimethoprim. Using 1,2,3-trimethoxybenzene as the parent compound and considering the free energy of solvation of all other methoxybenzenes (and benzene) relative to it, Kuyper et al. found the relative free energy of solvation to be, in increasing order of methoxy substitution, $\Delta\Delta G_{solv}$ = 1.68 kcal/mol (1,2,3-trimethoxybenzene → 1,2-dimethoxybenzene), 3.03 kcal/mol (1,2,3-trimethoxybenzene → anisole) and 4.54 kcal/mol (1,2,3-trimethoxybenzene → benzene),[11] and these are reproduced in Table III. This trend is similar to what we observe but appears to be much more additive. Specifically, the incremental change in free energy from the trimethoxy compound to that with only two methoxy groups is 1.68 kcal/mol for the benzenes and 2.0 kcal/mol for the trimethoprim-related compounds. Similarly, the difference between 1,2,3-trimethoxybenzene and benzene is 4.54 kcal/mol compared to about 4 kcal/mol for trimethoprim and the triethyl derivative. The deviations between the benzenes and ethyl-substituted congeners of TMP are greatest for the disubstituted species. This is where one might expect the size and flexibility of the ethyl moieties, compared to simple hydrogen, to be manifest due to the interactions between the adjacent ethyl and methoxy groups as well as the increased hydrophobic surface area expected for an ethyl group compared to hydrogen. The effect of "pairing" when adjacent ethyl groups replace methoxy groups (compared with hydrogen replacing methoxy) is evident in the vacuum portions of the free energies found in Table II. Although these free energies by themselves (without reference to a closed thermodynamic cycle) are not physically meaningful, we see that ethyl substitution at adjacent sites is different from ethyl substitution at the 3′,5′ positions. Overall, however, we find that the incremental changes observed in our calculations compare very well to the experimental measurements on methoxybenzenes, and such a comparison provides a further test of our calculations.

IV. Conclusion

In this paper we have presented an extensive study of the aqueous solvation thermodynamics of all unique congeners of trimethoprim derived from the substitution of benzyl methoxy groups by ethyl moieties. Our calculations show anomalous (nonadditive) solvation free energies for the 3′,5′-diethyl-substituted derivative of trimethoprim and the triethyl-substituted one, illustrating the experimentally observed hydrophilicity of the *p*-methoxy group in substituted benzenes.[18] The origin of this effect is seen to be due to favorable (or near favorable) entropy contributions in aqueous solution. Thus, the juxtaposition of the methoxy group and two flanking ethyl groups on benzene leads to decreased water ordering and greater hydrophilicity.

We have compared our calculations with measurements of solvation free energies for methoxybenzenes. This comparison indicates that similar free energy changes (on the order of 2 kcal/mol per methoxy substitution) occur in both series of compounds and provides a good check on our calculations. The major differences observed between the congeners of trimethoprim and

(18) Anderson, G. M.; Kollman, P. A.; Domelsmith, L. N.; Houk, K. N. *J. Am. Chem. Soc.* **1979**, *101*, 2344.

the methoxybenzenes is the nonadditivity of incremental free energy changes in the trimethoprim series. We have ascribed these differences to the inherent differences between ethyl and hydrogen solvation thermodynamics and flexibility.

Finally, we note that this study paves the way for a detailed examination of "drug design" strategies by thermodynamic simulations, using as a prototypical system the binding of trimethoprim congeners to the enzyme dihydrofolate reductase. The presentation of these results and a discussion of their interpretation are forthcoming.

Acknowledgment. Support for this research from the NIH (Grant GM37554) is gratefully acknowledged. The computational resources necessary to carry out this work were made available through grants from the Pittsburgh Supercomputing Center, and acknowledgment is made to them for their support.

Spectroscopic Characterization of Lanthanide Octaethylporphyrin Sandwich Complexes. Effects of Strong $\pi\pi$ Interaction

John K. Duchowski and David F. Bocian*

Contribution from the Department of Chemistry, Carnegie Mellon University, Pittsburgh, Pennsylvania 15213. *Received September 25, 1989*

Abstract: Optical absorption and resonance Raman spectra are reported for the lanthanide sandwich porphyrins, $Eu^{III}(OEP)_2$, $Nd^{III}(OEP)_2$, and $La^{III}(OEP)_2$ (OEP = octaethylporphyrin). These complexes contain a single hole in the porphyrin π system and are electronically similar to the Ce^{IV} sandwich porphyrin cation radical $Ce^{IV}(OEP)_2^+$. Variable-temperature (10–300 K) UV–vis and near-infrared (NIR) spectra are obtained for all four single-hole sandwiches. At high resolution and/or at low temperatures, well-resolved fine structure is observed on the intradimer charge-transfer bands (ca. 1250 nm) of all the complexes. The absorption is dominated by a single Franck–Condon active vibration. This vibration is assigned as a mode, Q_{AB}, which contains a significant amount of multicenter character and modulates interring separation. Vibronic analysis of the NIR band contours reveals that two system origins, separated by 400–700 cm^{-1} (depending on the complex), are present. The progressions built off the lower and higher energy origins exhibit spacings of ~250 and ~315 cm^{-1}, respectively. The existence of two forms which differ in the relative orientation of their ethyl groups is suggested as the source of the double origin in the NIR region. The vibronic analysis indicates that the frequencies of the Q_{AB} modes of either form are ~120 cm^{-1} higher in the ground electronic state than in the charge-transfer excited state. The dimensionless origin shifts, Δ, along Q_{AB} are similar (although not exactly identical) for the two forms and range from 2.6 to 3.0 depending on the complex. These values of Δ correspond to differences in interring separation of ~0.05 Å between the ground and charge-transfer excited states. Collectively, the spectroscopic data indicate that the holes of all the sandwich complexes are delocalized over both rings on the vibrational and electronic time scales and that approximately 1/4 to 1/3 of the intradimer bonding in the ground electronic state can be attributed to $\pi\pi$ interaction.

I. Introduction

Photosynthetic proteins and certain organic conductors share the common feature of closely spaced porphyrinic π systems.[1-5] Strong electronic interactions between molecules within these natural and synthetic aggregates impart unique electron transfer and/or conductivity properties to the systems.[1,2,6-12] A necessary first step in understanding the functional behavior of these complicated assemblies is the characterization of the general electronic properties of strongly interacting porphyrinic species.[10,14-18] In this regard, we previously reported an investigation of $\pi\pi$ interactions in the lanthanide porphyrin sandwich complexes, $Ce^{IV}(OEP)_2$ and $Ce^{IV}(TPP)_2$ (OEP = octaethylporphyrin; TPP = tetraphenylporphyrin), as well as their corresponding π cation radicals.[19] These complexes are of particular interest because

(1) Okamura, M. Y.; Feher, G.; Nelson, N. In *Photosynthesis: Energy Conversion by Plants and Bacteria*; Academic Press: New York, 1982; Vol. 1, pp 195–272.
(2) Hoffman, B. M.; Ibers, J. A. *Acc. Chem. Res.* **1983**, *16*, 15–21, and references therein.
(3) (a) Diesenhofer, J.; Epp, O.; Miki, K.; Huber, R.; Michel, H. *J. Mol. Biol.* **1984**, *180*, 385–398. (b) Diesenhofer, J.; Epp, O.; Miki, K.; Huber, R.; Michel, H. *Nature* **1985**, *318*, 618–624.
(4) Chang, C.-H.; Tiede, D.; Tang, J.; Smith, U.; Norris, J.; Shiffer, M. *FEBS Lett.* **1986**, *205*, 82–86.
(5) Allen, J. P.; Feher, G.; Yeates, T. O.; Komiya, H.; Rees, D. C. *Proc. Natl. Acad. Sci. U.S.A.* **1987**, *84*, 5730–5734.
(6) (a) Martinsen, J.; Stanton, J. L.; Greene, R. L.; Tanaka, J.; Hoffman, B. M.; Ibers, J. A. *J. Am. Chem. Soc.* **1985**, *107*, 6915–6920. (b) Ogawa, M. Y.; Martinsen, J.; Palmer, S. M.; Stanton, J. L.; Tanaka, J.; Green, R. L.; Hoffman, B. M.; Ibers, J. A. *Ibid.* **1987**, *109*, 1115–1121.
(7) Turek, P.; Petit, P.; Andrē, J.-J.; Simon, J.; Even, R.; Boudjema, B.; Guillaud, G.; Maitrot, M. *J. Am. Chem. Soc.* **1987**, *109*, 5119–5122.
(8) Nohr, R. S.; Kuznesof, P. M.; Wynne, K. J.; Kenney, M. E.; Siebenman, P. G. *J. Am. Chem. Soc.* **1981**, *103*, 4371–4377.
(9) Diel, B. N.; Inabe, T.; Lyding, J. W.; Schoch, K. F., Jr.; Kannewurf, C. R.; Marks, T. J. *J. Am. Chem. Soc.* **1983**, *105*, 1551–1567.
(10) Pietro, W. J.; Marks, T. J.; Ratner, M. A. *J. Am. Chem. Soc.* **1985**, *107*, 5387–5391.
(11) Diel, B. N.; Inabe, T.; Taggi, N. K.; Lyding, J. W.; Schneider, O.; Hanack, M.; Kannewurf, C. R.; Marks, T. J.; Schwartz, L. H. *J. Am. Chem. Soc.* **1984**, *106*, 3207–3214.
(12) Collman, J. P.; McDevitt, J. T.; Leidner, C. R.; Yee, G. T.; Torrance, J. B.; Little, W. A. *J. Am. Chem. Soc.* **1987**, *109*, 4606–4614.
(13) Hale, P. D.; Pietro, W. J.; Ratner, M. A.; Ellis, D. E.; Marks, T. J. *J. Am. Chem. Soc.* **1987**, *109*, 5943–5947.
(14) Gouterman, M.; Holten, D.; Lieberman, E. *Chem. Phys.* **1977**, *25*, 139–153.
(15) Hunter, C. A.; Sanders, J. K. M.; Stone, A. J. *Chem. Phys.* **1989**, *133*, 395–404.
(16) Schick, G. A.; Schreiman, I. C.; Wagner, R. W.; Lindsey, J. S.; Bocian, D. F. *J. Am. Chem. Soc.* **1989**, *111*, 1344–1350.
(17) Osuka, A.; Maruyama, K. *J. Am. Chem. Soc.* **1988**, *110*, 4454–4456.
(18) (a) Yan, X.; Holten, D. *J. Phys. Chem.* **1988**, *92*, 409–414. (b) Bilsel, O.; Rodriguez, J.; Holten, D. *J. Phys. Chem.* Submitted for publication.
(19) Donohoe, R. J.; Duchowski, J. K.; Bocian, D. F. *J. Am. Chem. Soc.* **1988**, *110*, 6119–6124.

0002-7863/90/1512-3312$02.50/0